Macromolecules
ARTICLE

Macromolecules **2010**, *43*, 3817–3827 **3817**
DOI: 10.1021/ma902782x

Indanedione-Substituted Poly(terthiophene)s: Processable Conducting Polymers with Intramolecular Charge Transfer Interactions

Klaudia Wagner,[†] Loretta L. Crowe,[‡] Pawel Wagner,[†] Sanjeev Gambhir,[†] Ashton C. Partridge,[‡] John C. Earles,[§] Tracey M. Clarke,[§] Keith C. Gordon,[§] and David L. Officer*[,†]

[†]*The ARC Centre of Excellence for Electromaterials Science, Intelligent Polymer Research Institute, University of Wollongong, Innovation Campus, Squires Way, Fairy Meadow, NSW 2519, Australia,* [‡]*IFS MacDiarmid Centre, Massey University, Private Bag 11-222, Palmerston North, New Zealand, and* [§]*The MacDiarmid Institute for Advanced Materials and Nanotechnology and Chemistry Department, University of Otago, Dunedin, New Zealand*

Received December 17, 2009; Revised Manuscript Received March 12, 2010

ABSTRACT: The electrochemical and chemical syntheses of poly(terthiophene)s bearing an indanedione pendant group and displaying intramolecular charge transfer interactions have been achieved. The nature of the charge transfer interaction is characterized through DFT calculations and experimental studies, including resonance Raman spectroscopy and absorption and emission data through a Lippert−Mataga analysis. It is found that the low-energy transition present in the indanedione-bearing monomer species has considerable charge transfer character with a dipole change of 11 D. Decomposition of the indanedione group occurred during hydrazine reduction after chemical polymerization. A soluble, low molecular weight indanedione-substituted polymer (weight average 4500 Da) was nonetheless obtained following the use of a milder reducing agent, triethanolamine. To the best of our knowledge, this is the first example of the use of triethanolamine for the reduction of an oxidized polythiophene, providing a milder and safer alternative to hydrazine. In an attempt to produce higher molecular weight processable polymers with intramolecular charge transfer interactions, a copolymer of the indanedione-substituted terthiophene and a dihexylterthiophene was synthesized. The electronic conjugation of the produced polymers was characterized by Raman frequency dispersion experiments and show dispersion rate parameters similar to those observed for other substituted polythiophenes.

Introduction

Polythiophene derivatives are of particular interest due to their stability and relative ease of synthesis and functionalization.[1] They can be applied in a broad range of devices: from simple solar cells[2] to complex electroluminescent devices.[3,4] The electronic character of attached functional groups typically affects the electron density of the thiophene rings in the polymer. The energy gap E_g is related to the electrical and optical properties of the polymer and has often been lowered by extending the π-electron delocalization over the whole backbone chain or by using electron donors or electron acceptors as substituents, which induce minimally twisted arrangements in the conjugated polymers.[4] This kind of donor-π-acceptor (D-π-A) arrangement in oligomers or polymers can permit a high degree of intramolecular charge transfer (ICT).[5−8] ICT interaction can provide low-band-gap polymers with broad absorption bands that extend into the near-infrared spectral range, high electron affinity and low ionization potential, efficient photoinduced charge transfer and separation, and ambipolar charge transport with high mobility.[9,10]

Strongly electron-accepting groups can considerably enhance the absorption characteristics of the monomer or polymer they are attached to and may also induce an ICT with the potential to facilitate charge separation of excitons formed when the compound is exposed to light.[9] Recently, Roquet et al. report a study on triphenylamine−thienylenevinylene hybrid systems with internal charge transfer as donor materials for heterojunction solar cells.[8] This demonstrated that an extension of photoresponse in the visible spectral region, an increase of the maximum external quantum efficiency, and an increase of the open-circuit voltage under white light illumination could be offered using ICT materials.

Neutral polythiophene and its simple functionalized derivatives have a narrow absorbance range (350−550 nm). With the addition of more complex pendant groups, such as dicyanoethene[6] or indanedione, the absorbance spectrum of the polymer can be extended into the visible region. This is typically the approach taken to improve the light-harvesting capability and increase the efficiency of polymer solar cells.[2] However, to the best of our knowledge, there are no reports of the use of polymers with well-developed ICT interactions to enhance photovoltaic efficiency. Part of the challenge in this regard is development of suitably functionalized polythiophene that are readily processable to make such devices.

In this paper, we have investigated the chemical and electrochemical polymerization of terthiophenes modified at the 3′-position with the electron-accepting 1,3-indanedione group. Terthiophene was chosen as the monomer to ensure that the bulky indanedione substituent did not substantially affect the conformation of the polythiophene backbone. Alkoxy groups were introduced at the 4- and 4″-positions on the outer thiophene rings, in order to not only provide donor character to the polymer but also improve the polymer processability. In addition, 4-alkoxy substitutions activate the 5-position for oxidation, ensuring longer

*To whom correspondence should be addressed. E-mail: davido@uow.edu.au.

Published on Web 03/26/2010

and more regioregular polymers with correspondingly high conductivity.[11] In order to explore the processability of polymers with intramolecular charge transfer interactions, copolymers of the indanedione-substituted terthiophene and a dihexylterthiophene were synthesized. The electrochemically polymerized homopolymers of the indanedione terthiophenes showed promise for expanding the range of light absorbance in polythiophenes, but they suffer from a lack of processability. In contrast, chemical polymerization using judicious reduction afforded a processable polymer, which retained the ICT interactions. In an attempt to increase the molecular weight of this chemically soluble polymer, copolymers of the indanedione-substituted terthiophene and a dihexylterthiophene were also successfully synthesized.

Experimental Section

Materials and Methods. All solvents were supplied by Merck and were used as received without further purification. The building blocks, 3,4-dihexylthiophene,[12] 2,5-dibromo-3,4-dihexylthiophene,[12] 2,5-dibromo-3-thiophenecarboxaldehyde,[13] 4-hexyloxy-2-thienylboronic acid, and 4-decyloxy-2-thienylboronic acid,[14] were synthesized according to literature procedures. Terthiophene-3′-aldehyde (**1c**) was synthesized according to the method of Collis et al.[15] Other reagents used in the syntheses and polymerizations were obtained from commercial sources.

^{1}H NMR spectra were recorded on Bruker Avance 400 and 500 spectrometers using TMS as an internal standard. In some cases not all carbon resonances were resolved due to the overlap of peaks. UV spectra were recorded in chloroform on a Shimadzu UV-3101PC UV/vis/NIR scanning spectrophotometer controlled by a PC running Shimadzu software. FT-IR spectra were obtained on a Nicolet 5700 FT-IR under argon flow. FAB$^+$ mass spectra were collected by the University of Auckland Mass Spectrometry Centre, while MALDI-TOF mass spectra were obtained in-house on a Micromass Maldi system (linear mode, terthiophene matrix). Molecular weight measurement of the soluble fraction of the chemical polymerization was carried out using gel permeation chromatography (GPC) on a Shimadzu LC-10AT liquid chromatograph equipped with a Phenogel 5 μm (10^4 Å porosity) column of 300 mm in length. Chromatographic grade tetrahydrofuran was used as an eluent. Calibration was done with a series of polystyrene standards (M_w range of 376−513 000 Da).

All electrochemical measurements were performed in a three-electrode cell, with a nonaqueous Ag/Ag$^+$ reference electrode and Pt mesh counter electrode. The polished platinum disk (0.021 cm^2, Bioanalytical Systems) was used as the working electrode. The spectroscopic measurements of the polymer films deposited on ITO (indium tin oxide) electrode were carried out on the earlier-mentioned Shimadzu UV-3101PC UV/vis/NIR scanning spectrophotometer. An Autolab potentiostat controlled by a PC running the Autolab GPES software system was used for cyclic voltammetry. The spectroelectrochemisty of the polymer films was investigated in solutions of 0.1 M tetrabutylammonium perchlorate (TBAP) in acetonitrile over applied voltages of 0.0 to 1.2 V (vs Ag wire). These voltages were then rescaled to −0.4 to 0.8 V (vs Ag/Ag$^+$).

SEM analysis was performed using a Cambridge 250Mk3 scanning electron microscope in secondary mode.

Synthesis of 4,4″-Dihexyloxy[2,2′;5′,2″]terthiophene-3′-carboxaldehyde (1a). In separate flasks, an aqueous (20.0 mL) solution of potassium carbonate (2.46 g) and a 1,2-dimethoxyethane (30 mL) solution of 2,5-dibromo-3-thiophenecarboxaldehyde (0.68 g, 2.50 mmol) and 4-hexyloxy-2-thienylboronic acid (2.28 g, 10.00 mmol) were prepared. After degassing the contents of both flasks under argon for 30 min, the two solutions were combined, and tetrakis(triphenylphosphine)palladium catalyst (0.36 g) was added to the resulting mixture. The reaction mixture was then held at reflux overnight with rapid stirring. After cooling to room temperature, the mixture was diluted with Et_2O and washed with distilled water. The organic phase was then dried over $MgSO_4$ and the solvent removed under vacuum. The ensuing red-brown oil was purified by column chromatography (silica gel, 10% CH_2Cl_2 in hexane), resulting in **1a** as an orange oil (0.77 g, 64% yield). ^{1}H NMR (400 MHz, $CDCl_3$): δ 10.04 (s, 1H, CHO), 7.47 (1H, H4), 6.94 (d, 1H, J = 1.5 Hz, H3′), 6.84 (d, 1H, J = 1.5 Hz, H3″), 6.36 (d, 1H, J = 1.5 Hz, H5′), 6.15 (d, 1H, J = 1.5 Hz, H5″), 3.95−3.90 (m, 4H, O−CH_2), 1.77−1.72 (m, 4H, Alk), 1.48−1.37 (m, 4H, Alk), 1.36−1.25 (m, 8H, Alk), 0.92−0.83 (m, 6H, CH_3). ^{13}C NMR (100 MHz, $CDCl_3$): δ 184.9, 157.8, 157.7, 146.0, 137.7, 136.9, 133.8, 130.4, 122.1, 121.3, 117.2, 100.7, 97.5, 32.3, 30.9, 30.8, 29.7, 29.6, 23.1, 14.5. UV−vis ($CHCl_3$) λ_{max} nm/(ε): 335 (29 000). FT-IR: cm^{-1} 3117, 2917, 2855, 1674, 1575, 1555, 1526, 1473, 1454, 1400, 1380, 1224, 1185, 1171, 1160, 1030, 962, 830, 720. MS (EI$^+$): m/z 476 (100%), 392 (9%), 308 (24%), 280 (16%), 43 (36%). HRMS (EI$^+$): found: 476.1512; calcd for $C_{25}H_{32}O_3S_3$: 476.1514.

Synthesis of 4,4″-Didecyloxy[2,2′;5′,2″]terthiophene-3′-carboxaldehyde (1b). In separate flasks, an aqueous (48.0 mL) solution of potassium carbonate (6.01 g) and a 1,2-dimethoxyethane (80 mL) solution of 2,5-dibromo-3-thiophenecarboxaldehyde (1.84 g, 6.86 mmol) and 4-decyloxy-2-thienylboronic acid (4.58 g, 16.10 mmol) were prepared. After degassing the contents of both flasks under argon for 30 min, the two solutions were combined, and tetrakis(triphenylphosphine)palladium catalyst (1.08 g) was added to the resulting mixture. The reaction mixture was then held at reflux overnight with rapid stirring. After cooling to room temperature, the mixture was diluted with Et_2O and washed with distilled water. The organic phase was then dried over $MgSO_4$ and the solvent removed under vacuum. The ensuing red-brown oil was purified by column chromatography (silica gel, 10% CH_2Cl_2 in hexane), resulting in an orange oil, which solidified to give **1b** as a dark red-brown solid (2.48 g, 4.21 62% yield) upon standing; mp: 51−53 °C. ^{1}H NMR (400 MHz, $CDCl_3$): δ 10.04 (s, 1H, CHO), 7.47 (s, 1H, H4), 6.93 (d, 1H, J = 1.5 Hz, H3′), 6.83 (d, 1H, J = 1.5 Hz, H3″), 6.35 (d, 1H, J = 1.5 Hz, H5′), 6.14 (d, 1H, J = 1.5 Hz, H5″), 4.01−3.97 (m, 4H, OCH_2), 1.83−1.94 (m, 4H, Alk), 1.78−1.62 (m, 28H, Alk), 1.46−1.43 (m, 6H, CH_3). ^{13}C NMR (100 MHz, $CDCl_3$): δ 157.9, 157.7, 146.1, 137.7, 137.0, 133.8, 130.5, 122.2, 121.3, 117.2, 100.7, 97.6, 70.4, 70.2, 31.9, 29.6, 29.4, 29.3, 29.2, 26.1, 22.7, 14.2. FT-IR: cm^{-1} 714, 822, 959, 1034, 1159, 1171, 1184, 1223, 1383, 1398, 1454, 1473, 1527, 1558, 1572, 1674, 2854, 2918, 3116. UV−vis ($CHCl_3$) λ_{max} nm/(ε): 335 (32 000), 375 (32 000). MS (EI$^+$): m/z 588(100%), 308 (12%), 280 (10%), 235 (8%), 57 (15%), 43 (39%). HRMS (EI$^+$): found: 588.2761; calcd for $C_{33}H_{48}O_3S_3$: 588.2767.

Synthesis of 2-(4,4″-Hexyloxy[2,2′;5′,2″]terthiophen-3′-ylmethylene)indan-1,3-dione (2). A tetrahydrofuran (6.0 mL) solution was prepared with 4,4″-bis(hexyloxy)[2,2′;5′,2″]terthiophene-3′-carboxaldehyde (0.203 g, 0.440 mmol) and 1,3-indanedione (71 mg, 0.49 mmol). Addition of piperidine (0.5 mL) caused the solution to darken to a deep red-black in color. The reaction solution was stirred at room temperature overnight, then was diluted with Et_2O (50 mL), and washed with diluted hydrochloric acid. The organic phase was separated, dried over magnesium sulfate, and evaporated to dryness. The resulting red oil was redissolved in a minimum amount of chloroform and precipitated by cold methanol to give **2** as a red powder (0.216 g, 81%); mp: 101−103 °C. ^{1}H NMR (400 MHz, $CDCl_3$): δ 8.66 (s, 1H, H4), 8.03 (s, 1H, CH), 8.02−7.94 (m, 2H, Ar−H), 7.78−7.73 (m, 2H, Ar−H), 6.93 (d, 1H, J = 1.5 Hz, H-3′), 6.88 (d, 1H, J = 1.5 Hz, H4″), 6.38 (d, 1H, J = 1.5 Hz, H5′), 6.20 (d, 1H, J = 1.5 Hz, H5″), 3.97−3.91 (m, 4H, O−CH_2), 1.78−1.71 (m, 4H, Alk), 1.50−1.39 (m, 4H, Alk), 1.38−1.23 (m, 8H, Alk), 0.95−0.84 (m, 6H, CH_3). ^{13}C NMR (100 MHz, $CDCl_3$): δ 158.3, 157.8, 147.2, 142.5, 140.4, 136.1, 135.7, 135.2, 134.9, 134.3, 132.0, 127.5, 123.2, 117.1, 101.2, 97.3, 32.3, 30.9, 30.8, 29.7, 29.6, 23.1, 14.5. FT-IR: cm^{-1} 3105, 2920, 2858, 1729, 1690, 1601, 1587, 1568, 1475, 1345, 1222, 1186, 1034, 737. UV−vis ($CHCl_3$) λ_{max} nm/(ε): 350 (62 000), 467 (14 000). MS (EI$^+$): m/z 604 (100%), 425 (15%), 324 (8%), 285 (15%), 57 (11%), 43 (41%). HRMS (EI$^+$): found: 604.1784; calcd for $C_{34}H_{36}O_4S_3$: 604.1776.

Synthesis of 2-(4,4″-Didecyloxy[2,2′;5′,2″]terthiophen-3′-ylmethylene)indan-1,3-dione (3). A tetrahydrofuran (10.0 mL) solution was prepared with 4,4″-bis(decyloxy)[2,2′;5′,2″]terthiophene-3′-carboxaldehyde (0.249 g, 0.423 mmol) and 1,3-indanedione (79.1 mg, 0.541 mmol). Addition of piperidine (0.5 mL) caused the solution to darken to a deep red-black in color. The reaction solution was stirred at room temperature overnight and then run through a short silica gel column with pure CH_2Cl_2. The resulting crude oil was suspended in a minimal amount of Et_2O and chilled over ice. The solids were then filtered off, washed with cold Et_2O, and dried, giving **3** as a bright orange powder (0.187 g, 0.260 mmol, 62% yield); mp: 82−85 °C. ^{1}H NMR (500 MHz, $CDCl_3$): δ 8.64 (s, 1H, H4), 8.01 (s, 1H, CH), 8.00−7.95−8.00 (m, 2H, Ar), 7.80−7.75 (m, 2H, Ar), 6.94 (d, 1H, J = 1.5 Hz, H3′), 6.89 (d, 1H, J = 1.5 Hz, H3″), 6.41 (d, 1H, J = 1.5 Hz, H5′), 6.19 (d, 1H, J = 1.5 Hz, H5″), 4.03−3.94 (m, 4H, OCH_2), 1.84−1.74 (m, 4H, Alk), 151−1.42 (m, 4H, Alk), 139−1.22 (m, 24H, Alk), 0.92−0.86 (m, 6H, CH_3). ^{13}C NMR (100 MHz, $CDCl_3$): δ 158.2, 157.7, 147.4, 142.5, 140.3, 136.2, 135.9, 135.2, 135.0, 134.4, 131.9, 127.4, 123.2, 121.4, 117.0, 101.3, 97.5, 70.4, 70.2, 31.9, 29.6, 29.4, 29.3, 29.2, 26.0, 22.7, 14.1. FT-IR: cm^{-1} 3103, 2918, 2852, 1726, 1687, 1603, 1585, 1570, 1473, 1348, 1219, 1190, 1171, 1036, 731. UV−vis ($CHCl_3$) λ_{max} nm/(ε): 350 (46 000), 467 (12 000). MS (EI$^+$): m/z 716 (100%), 0.447 (12%), 308 (18%), 146 (11%), 111 (17%). HRMS (EI$^+$): found: 716.3048; calcd for $C_{42}H_{52}O_4S_3$: 716.3028.

Synthesis of 4,4″-Didecyloxy-3′,4′-dihexyl[2,2′;5′,2″]terthiophene (6). In separate flasks, an aqueous (46.0 mL) solution of potassium carbonate (6.03 g) and a 1,2-dimethoxyethane (80 mL) solution of 2,5-dibromo-3,4-dihexylthiophene (2.31 g, 5.63 mmol) and 4-decyloxy-2-thienylboronic acid (4.01 g, 14.1 mmol) were prepared. After degassing the contents of both flasks under argon for 30 min, the two solutions were combined, and tetrakis-(triphenylphosphine)palladium catalyst (0.87 g) was added to the resulting mixture. The reaction mixture was then held at 80 °C overnight with rapid stirring. After cooling to room temperature, the mixture was diluted with Et_2O and washed with distilled water. The organic phase was then dried over $MgSO_4$ and the solvent removed under vacuum. The ensuing red-brown oil was purified by column chromatography (silica gel, 25% CH_2Cl_2 in hexane), resulting in an amber oil, which solidified upon standing. The oil was suspended in hexane, which caused a yellow solid byproduct to precipitate. After removing the byproduct by filtration, the filtrate was concentrated under vacuum to form dark amber oil, which solidified to a waxy, low-melting solid **6** upon standing (2.94 g, 4.03 mmol, 71.6% yield). ^{1}H NMR (500 MHz, $CDCl_3$): δ 0.92−0.96 (m, 12H), 1.33−1.37 (m, 34H), 1.44−1.51 (m, 6H), 1.56−1.63 (m, 4H), 1.79−1.85 (m, 4H), 2.70−2.74 (m, 4H), 3.99 (t, 4H, J = 6.6 Hz), 6.20 (d, 2H J = 1.7 Hz), 6.79 (d, 2H, J = 1.7 Hz). ^{13}C NMR (500 MHz, $CDCl_3$): δ 14.11, 14.15, 22.68, 22.73, 26.11, 26.97, 28.09, 29.31, 29.38, 29.46, 29.62, 29.63, 30.79, 31.56, 31.95. FT-IR: cm^{-1} 621, 685, 818, 868, 1026, 1171, 1363, 1466, 1533, 1554, 2854, 2923. UV−vis ($CHCl_3$) λ_{max} nm/(ε): 266 (11 800), 345 (13 600). MS (FAB$^+$): m/z 728 (100%), 729 (54%), 730 (23%).

General Procedure for Chemical Polymerization of Functionalized Terthiophenes. In separate flasks, 1 equiv of monomer (ca. 50 mg) and 4 equiv of ferric chloride were dissolved in $CHCl_3$ (6.0 mL each) and degassed under argon for 30 min. The monomer solution was then chilled down to −10 °C in an ice/salt bath, and the $FeCl_3$ slurry was added in dropwise fashion over 25 min under argon flow. After addition of the catalyst, the mixture was allowed to warm up to room temperature and left stirring overnight. The insoluble oxidized polymer was then filtered off, washed with water, and dried in air. After grinding the dried polymer to a fine powder with a mortar and pestle, it was reduced by addition of 10.0 mL of triethanolamine and 20.0 mL of chlorobenzene and heated at 80 °C for 3 h. The organic layer and undissolved polymeric solids were washed repeatedly with distilled water, and the chlorobenzene solvent was removed under vacuum. The resulting solids were then filtered, washed repeatedly with water, and subjected to successive Soxhlet extractions with methanol, acetone, hexane, dichloromethane, and finally $CHCl_3$. The $CHCl_3$ fraction was dried under vacuum, giving the polymer as a maroon to dark purple solid. In case of **poly-6**, reduction of polymer after the chemical polymerization of monomer was done using aqueous hydrazine (1.5−2.0%) and chloroform extraction at reflux for 3 h. The organic layer was separated. Solvent removal resulted in the reduced polymer, which was purified by successive Soxhlet extractions with methanol, acetone, and finally with $CHCl_3$. The fraction eluted with $CHCl_3$ resulted in a dark maroon solid (**poly-6**).

Chemical Homopolymerization of Poly[2-(4,4″-didecyloxy-[2,2′;5′,2″]terthiophen-3′-ylmethylene)indan-1,3-dione] (Poly-3c). The polymer ($CHCl_3$ fraction) was collected as a dark purple solid (34.0 mg) from 2-(4,4″-bis(decyloxy)[2,2′;5′,2″]terthiophen-3′-ylmethylene)indan-1,3-dione (50.4 mg, 0.0703 mmol). FT-IR: cm^{-1} 540, 582, 733, 796, 943, 1066, 1088, 1153, 1200, 1331, 1348, 1367, 1384, 1454, 1504, 1560, 1576, 1599, 1682, 1722, 2850, 2922. MALDI-MS (terthiophene): m/z 1429 (2%), 2144 (100%), 2859 (21%), 3575 (8%), 4292 (11%), 5008 (3%), 5726 (1%), 6445 (1%). GPC (polystyrene): M_w 4500 Da; PDI = 1.5.

Chemical Homopolymerization of Poly[4,4″-didecyloxy-3′,4′-dihexyl[2,2′;5′,2″]terthiophene] (Poly-6). The polymer ($CHCl_3$ fraction) was collected as a dark maroon solid (39.6 mg) from 4,4″-bis(decyloxy)-3′,4′-dihexyl[2,2′;5′,2″]terthiophene (49.4 mg, 0.0677 mmol). ^{1}H NMR (500 MHz, $CDCl_3$): δ 6.90 (br s, 2H), 4.15 (br s, 4H), 2.76 (br s, 4H), 0.84−1.91 (multiple peaks, 60 H). FT-IR: cm^{-1} 721, 796, 1066, 1190, 1261, 1352, 1385, 1408, 1429, 1458, 1514, 1624, 2852, 2924. GPC (polystyrene): M_w 91 300 Da; PDI = 1.8.

Chemical Copolymerization of Poly[4,4″-didecyloxy-3′,4′-dihexyl[2,2′;5′,2″]-terthiophene-*co*-2-(4,4″-didecyloxy[2,2′;5′,2″]-terthiophen-3′-ylmethylene)indan-1,3-dione] (Poly-3/6). The copolymer ($CHCl_3$ fraction) was collected as a dark maroon/purple solid (34.2 mg) from 4,4″-bis(decyloxy)-3′,4′-dihexyl[2,2′;5′,2″]-terthiophene (25.4 mg, 0.0346 mmol) and 2-(4,4″-bis(decyloxy)-[2,2′;5′,2″]terthiophen-3′-ylmethylene)indan-1,3-dione (24.8 mg, 0.0348 mmol). FT-IR: cm^{-1} 540, 584, 719, 733, 798, 945, 1066, 1153, 1190, 1261, 1348, 1385, 1408, 1458, 1512, 1576, 1599, 1682, 1713, 2852, 2922. GPC (polystyrene): M_w 20 400 Da; PDI = 2.6.

Electrochemical Homopolymerization of Poly[2-(4,4″-didecyloxy-[2,2′;5′,2″]terthiophen-3′-ylmethylene)indan-1,3-dione] (Poly-3e). Polymer films were electrochemically grown on optically transparent ITO-coated glass by chronoamperometric deposition at constant potential (0.9 V, 50 s) from a solution of 0.1 M TBAP in CH_2Cl_2, containing the monomer at a concentration of 20 mM.

Conductivity Measurements. A four-point resistivity meter (Jandel model RM2), with spacing in square array 0.635 mm, was used in conductivity measurements. **Poly-2e** and **poly-3e** were electrochemically grown on optically transparent ITO-coated glass by chronoamperometric deposition at constant potential of 0.9 V for 1 h, from a solution of 0.1 M TBAP in CH_2Cl_2 containing the monomer at a concentration of 20 mM.

Computational Methods. DFT calculations were performed using the Gaussian03 package. On the basis of previous studies on similar thiophene-based compounds,[16−18] we used a Becke-style three-parameter method with the Lee−Parr−Yang correlation functional (B3LYP) and a 6-31G(d) basis set. Optimized geometries were used to calculate the vibrational spectra (IR and Raman) so that these could be compared to experimental data. Importantly, no imaginary frequencies were obtained, consistent with an energy minimum of rhte geometries provided. Frequencies were scaled by 0.970 prior to the calculation of mean absolute deviation (MAD) in frequency for those bands >10% the intensity of the strongest band in the region of interest (800−1650 cm^{-1}). In order to test the efficacy of the calculations, the predicted normal Raman spectrum was compared to the experimental data generated using 1064 nm excitation; for the bands of above weak intensity (>10% maximum band

Table 1. Experimental and Calculated (TDDFT) Electronic Spectral Data for Indanedione-Substituted Thiophene 5 and Terthiophenes 4 and 3

	experimental data		calculated data		
compound	λ/nm	$\varepsilon/10^3$ M^{-1} cm^{-1}	λ/nm	f	MO contributions (configuration coefficients)
5	363	15.0	332	0.25	62, 64 (−0.47); 62, 63 (0.44)
			320	0.53	60, 63 (0.50); 62, 63 (0.34)
4	457	10.3	492	0.16	104, 105 (0.66); 102, 105 (0.12)
	340	42.0	352	0.39	102, 105 (0.46); 103, 105 (−0.33); 101, 105 (−0.30)
			347	0.44	104, 107 (0.57); 102, 105 (0.26); 104, 107 (−0.26)
3	471	11.6	508	0.15	120, 121 (0.66)
	347	37.0	354	0.51	115, 121 (−0.13); 120, 123 (0.64)
			337	0.43	115, 121 (−0.18); 116, 121 (0.61); 119, 122 (−0.13)
$\mathbf{3}^+$			817	0.16	120, 121 (−0.46); 119, 120 (0.85)
			581	0.03	120, 121 (0.68); 119, 121 (0.23); 117, 120 (−0.42)

Scheme 1. Syntheses of Indandione-Substituted Monomers and Polymers

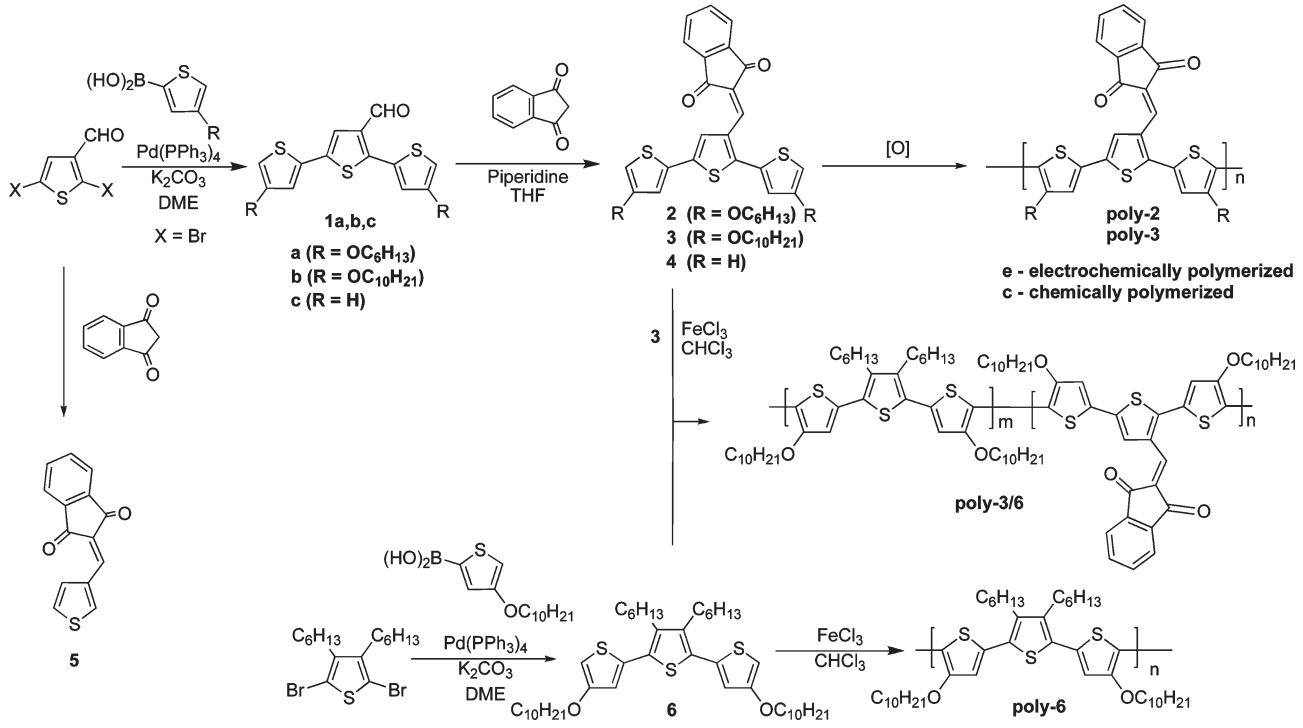

intensity) in the 800−1650 cm^{-1} region, the mean absolute deviations between predicted and observed frequencies are 6 cm^{-1} for **3**, 7 cm^{-1} for **4**, and 8 cm^{-1} for **5**; we consider this a good correlation.[16,18−20] The data for **3**, **4**, and **5** are given in Table 1 and Figure 2 (for **4**).

Raman Spectroscopy. Normal Raman spectra were recorded of powder samples using a Bruker Equinox-55 FT-interferometer bench with a FRA106/5 Raman accessory and utilizing OPUS v5.0 software. A Nd:YAG laser operating at 1064 nm provided excitation and a Ge diode (D418-T) functioning at liquid nitrogen temperature was used to collect the scattered Raman photons. Typically, 64 scans at 4 cm^{-1} resolution were taken at 100 mW laser power. No burning of sample was observed.

Resonance Raman spectra were recorded using a setup described previously.[21−24] Briefly, a continuous-wave krypton-ion laser (Innova I-302, Coherent, Inc.), solid-state 444 nm diode (Crystal Laser), solid-state 532 nm Nd:YAG (B&W Tec Inc.), helium−neon (Oplectra, Germany), or argon-ion laser (Melles Griot Omnichrome MAP-543) was used to generate resonance Raman scattering. Band-pass filters removed the ion plasma emission lines from the laser output. The laser output was adjusted to give between 5 and 10 mW at the sample. Wavenumber calibration was performed using Raman bands from a 1:1 (by volume) mixture of acetonitrile and toluene. Peak positions were reproducible to within 1 cm^{-1}. Spectra were obtained with a resolution of 3−5 cm^{-1}. Peak positions were reproducible to within 1−2 cm^{-1}. Spectra were obtained with a resolution of 5 cm^{-1}. Films were located in position with an $x-y-z$ adjustable stage; some care was taken to ensure burning of the film (observed optically or by signal degradation) was avoided. This was accomplished using low powers at the sample (10 mW). Raman band intensities were corrected for self-absorption, and throughput of the optical path and spectrograph, and detector sensitivity.[21,25,26]

Results and Discussion

Monomer Synthesis. The synthesis of the indanedione-functionalized terthiophene (TTh) monomers **2** and **3** required the preparation of the corresponding aldehydes **1a** ($R = OC_6H_{13}$) or **1b** ($R = OC_{10}H_{21}$) (Scheme 1). These were easily prepared by the Suzuki coupling route that we had previously developed for the synthesis of terthiophene-3′-aldehyde (**1c**)[15] and the corresponding 4-alkoxyboronic acids.[14] The indanedione-functionalized TTh monomers **2** and **3** were synthesized in 81% and 62% yield, respectively, from the corresponding aldehydes **1a** and **1b** via Knoevenagel condensations with 1,3-indanedione (Scheme 1). The spectral characteristics of both indanediones were similar so only those of **3** are discussed here.

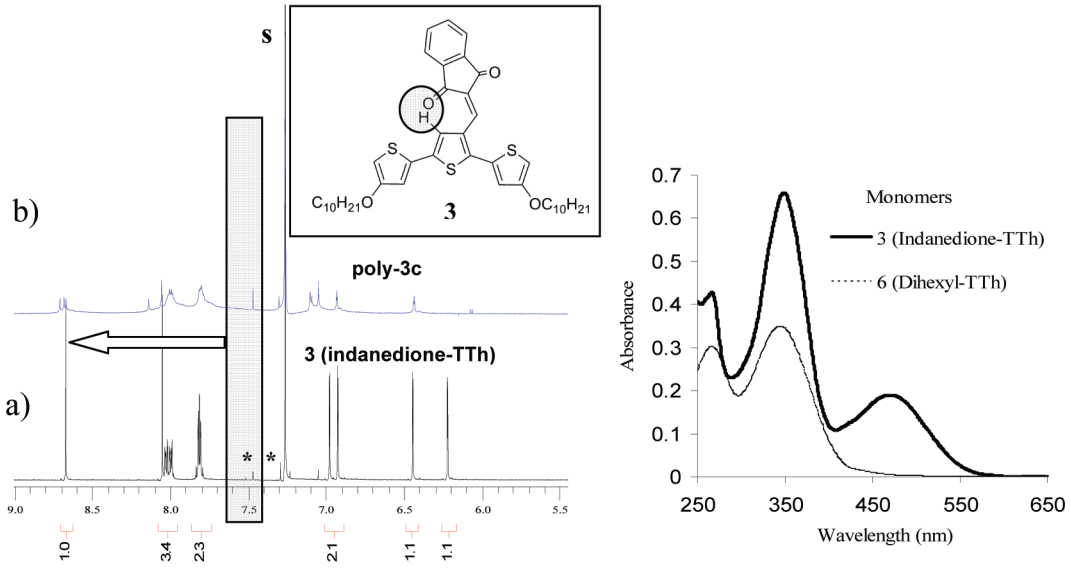

Figure 1. ^{1}H NMR spectra of (a) indanedione-TTh **3** and (b) polymeric indanedione-TTh **poly-3c** ($CDCl_3$, 500 MHz) and (c) the UV−vis spectra of the monomer **3** and dihexylterthiophene monomer **6**. The structure of the monomer **3** is also shown inset. The minor peaks indicated by * may be indicative of an alternative isomer; s = solvent.

The ^{1}H NMR spectrum of the indanedione−TTh **3** showed a sharp single proton signal at 8.6 ppm (Figure 1a), attributed to the hydrogen of the central thiophene ring, shifted considerably from its expected position at ~7.5 ppm (shaded box).[15] The shift likely results from the deshielding effect of the neighboring indanedione carbonyl group, suggesting that monomer **3** adopts the conformation shown in Figure 1 (inset), indicative of significant conjugative overlap between the terthiophene moiety and the indanedione substituent.

This is supported by the UV−vis spectrum of **3**, which exhibits two bands: the first at 353 nm, a typical terthiophene absorption band, and the second smaller absorption band at 471 nm, which we assign to an ICT band (Figure 1c), analogous to that observed previously for terthiophene indanedione,[10] as well as by Roquet et al. for a thiophene indanedione derivative.[8]

Two model indanedione monomers were also synthesized. The parent 3′-indanedioneterthiophene (**4**) itself was readily prepared from terthiophene-3′-aldehyde (**1c**) in 80% yield. We have reported some of the spectral properties of **4** previously.[10] The thiophene indanedione **5** was prepared according to a literature procedure.[27]

The synthesis of the second terthiophene monomer 4,4″-didecyloxy-3′,4′-dihexyl[2,2′;5′,2″]terthiophene (**6**) was readily achieved in 72% yield using a Suzuki coupling in an analogous fashion to that for aldehyde **1b** (Scheme 1). A similar monomer containing ethylenedioxythiophene units has been prepared by Melucci et al.[28] The syntheses of the homo- and copolymers of the three TTh monomers **2**, **3**, and **6** were then investigated.

Some insights into the electronic structure, particularly the ICT properties, of the monomers and their respective polymers may be gleaned from quantum calculations on these systems.[16,19] We have used density functional theory (DFT) to model the geometry, vibrational spectra, and electronic transitions of **3** and model compounds thereof. The structure calculated for **3** is consistent with the NMR data, with the carbonyl group on the indanedione moiety and the central thiophene hydrogen separated by about 2 Å. The structure (Figure S1) shows a deviation from planarity with respect to the ring systems; across the terthiophene backbone, planes, as defined by each thiophene ring, are angled 40° (for A and B) and 17° (for B and C) and the plane of the indanedione is almost planar to the central thiophene, 10° for planes B and D.

In order to examine the interaction between the indanedione and the thiophene backbone chain, two model compounds were studied using computational modeling and through analysis of spectroscopic properties. These compounds were thiophene−indanedione (**5**) and terthiophene−indanedione (**4**), which were compared to **3**. This series allows one to gauge the level of interaction as the thiophene system is extended form thiophene to terthiophene and the effect due to substitutents on the thiophene backbone. This interaction is readily observed in the electronic absorption spectra of the compounds, which may be modeled using time-dependent DFT. The experimental and calculated electronic absorption data are presented in Table 1. These data show a distinct trend; **5** has its lowest transition at 363 nm, corresponding to the calculated 332 nm transition, which involves the HOMO, LUMO and HOMO, LUMO+1 configurations. Analysis of these MOs reveals that they are delocalized across the entire structure, that is, they are not distinct indanedione or thiophene orbitals. For the terthiophene system **4**, a new transition is observed at 457 nm, predicted at 492 nm. The predicted transition is dominated by the HOMO−LUMO configuration, which shows distinct charge transfer character with the HOMO being terthiophene and LUMO indanedione in nature (Figure S2).

Further evidence for the charge transfer nature of the lowest energy transition of **4** is provided by an analysis of the shifts in transition energy for absorption and emission as a function of solvent.[29,30] Compound **4** is emissive in a variety of solvents and shows solvatochromic behavior. The shift in energy between the absorption and emission band, the so-called Stokes shift, may be related to the change in dipole moment on going from ground (μ_g) to excited state (μ_e).[31] Estimates of the dipole changes may be obtained experimentally using the Lippert−Mataga equation (1).[32] This relates the Stokes shift (ν_{st}, cm^{-1}) with the solvent polarity parameter (Δf), the Onsager radius of the fluorophores

of interest (a, m), and the fundamental constants (h, J s; ε_0, J^{-1} C^2 m^{-1}; and c, cm s^{-1}).

$$\nu_{st} = \frac{2(\mu_e - \mu_g)^2}{4\pi\varepsilon_0}\frac{\Delta f}{hca^3} + C \quad (1)$$

For the Onsager radius we have used the value of 6.4 Å, which is half of the long axis for the calculated structure of **4**. The solvent polarity parameter (Δf) is calculated from the dielectric constant (ε) and refractive index (n) of the solvent of interest as shown in eq 2.

$$\Delta f = \left(\frac{\varepsilon - 1}{2\varepsilon + 1}\right) - \left(\frac{n^2 - 1}{2n^2 + 1}\right) \quad (2)$$

The Lippert−Mataga plot, ν_{st} vs Δf (Figure S3), for **4** is linear ($R^2 = 0.93$) with a gradient of 5600 ± 1500 cm^{-1}. This observed linearity suggests that the large solvent-dependent shifts in the fluorescence spectrum are a consequence of the dipole−dipole interactions between solvent and solute.[33] From this analysis a value of $\Delta\mu = \mu_e - \mu_g = 11$ D is obtained. This shows that the transition has significant dipole change consistent with the charge transfer character of the transition. This value is comparable to that of CN-*pet* ($\Delta\mu = 12.5$ D), which also shows a characteristic charge transfer behavior.[29,34]

In addition, we have used resonance Raman spectroscopy to probe the nature of the lowest energy transition in **4**.

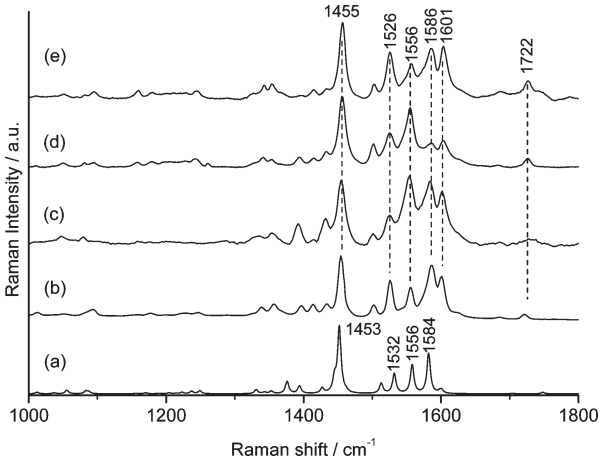

Figure 2. Raman spectra of **4**: (a) calculated spectrum; (b) FT-Raman (1064 nm excitation) on solid sample; (c) resonance Raman spectrum (excitation 351 nm) $CHCl_3$ solution; (d) resonance Raman spectrum (excitation 413 nm) $CHCl_3$ solution; (e) resonance Raman spectrum (excitation 457.9 nm) $CHCl_3$ solution.

Under the conditions of a resonance Raman experiment, the vibrational modes associated with the resonant chromophore are enhanced. These enhancements are distinct in that those vibrational modes that mimic the distortion caused by the resonant electronic transition are preferentially enhanced.[35] The normal Raman spectrum of **4** is dominated by a terthiophene stretch band[36,37] at 1455 cm^{-1} and additional features at 1526, 1556, 1586, and 1601 cm^{-1}, with a weak feature at 1722 cm^{-1}. The resonance Raman spectra (Figure 2c−e) show variations in spectral intensity on tuning from 351 to 457.9 nm excitation, consistent with the two differing electronic transitions present in the spectrum. With 457.9 nm (Figure 2e) excitation there is relative enhancement of the bands at 1601 and 1722 cm^{-1}. These bands are assigned as the stretch of the indanedione and the carbonyl stretch of the indanedione moiety. Enhancement of such bands is consistent with the TDDFT modeling of the low-energy transition in which the MO that acts as the acceptor orbital for this transition is based on the indanedione moiety.

The absorption spectrum of **3** shows a band at 471 nm, predicted at 508 nm, which, like that of **4**, has charge transfer character. In summary, the TDDFT calculations suggest that, with a polythiophene backbone, the lowest energy transition will likely be charge transfer in nature. This is also supported by analysis of the solvent-dependent absorption and emission data and the resonance Raman spectra of **4**.

Electrochemical Synthesis and Characterization. We have investigated the electrochemical polymerization of the two terthiophene monomers with OC_6H_{13} or $OC_{10}H_{21}$ alkoxy groups at the 4- and 4″-positions on the outer thiophene rings, **2** and **3**, respectively, and modified at the 3′-position with the 1,3-indanedione group. The electrochemical, spectroelectrochemical, and conductivity properties of the films were compared. The electrochemical growth of monomer **2** and its postpolymerization voltammograms are shown in Figure 3. Those of monomer **3** are similar and typical of other substituted terthiophenes.[38] Electropolymerization of **2** (Figure 3a) shows an increase in current with successive cycles indicative of electroactive film deposition. The post cyclic voltammogram (Figure 3b) exhibits broad reversible oxidation peaks at −0.22, 0.17, and 0.48 V characteristic of the typical doping and dedoping processes of polythiophene.[1] These types of voltammetric responses are associated with the complex mechanisms of charging−discharging processes taking place upon reverse cycling, which result from the transitions between the neutral, polaron, bipolaron, and metallic states of the polymer and involve structural reorganization and charging of the polymers fragments of different chain lengths.[39−41]

In order to examine the absorbance spectra of **poly-3e**, a film was grown on ITO under potentiostatic conditions (0.9 V),

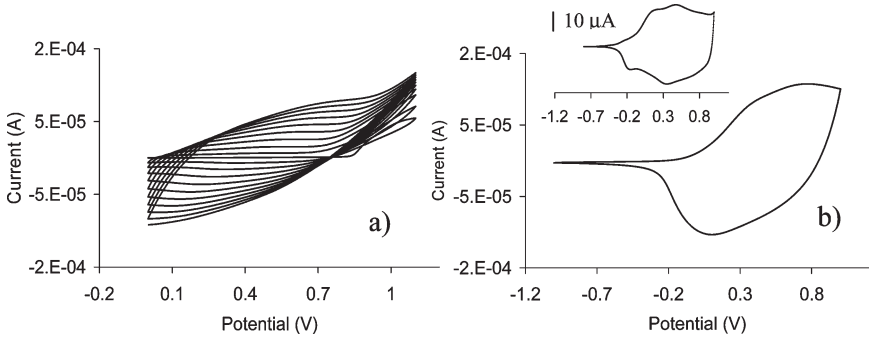

Figure 3. (a) Electrochemical polymerization and (b) post CV of **poly-2e**; scan rate 100 mV/s (inset: 10 mV/s).

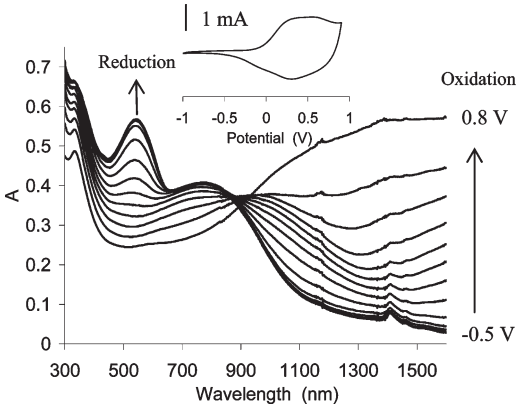

Figure 4. Spectroelectrochemistry of **poly-3e** (inset: post CV at 100 mV/s).

followed by post CV in acetonitrile to determine the electrical stability of the polymer film (Figure 4, inset). The spectroelectrochemical behavior of the film was investigated as the applied voltage was increased, thus oxidizing the polymer film. Electrochemical polymerization of the indanedione monomer resulted in a polymer exhibiting absorbances at 332, 540, and 778 nm in the neutral polymer (Figure 4). Upon oxidation, the electrochemically polymerized material developed a free carrier tail as well as exhibited a drop in absorbance at 332, 540, and 778 nm, as expected for an oxidized electroactive polythiophene.[42] The spectrum of the reduced polymer is almost identical to that reported by Gallazzi et al. for an analogous low molecular weight (M_n 3950) poly(alkoxyterthiophene) substituted with an electron-withdrawing dicyanoethenyl group.[7] While the spectrum is unassigned in this publication, the authors later postulate that the higher wavelength absorption peak in the UV−vis spectrum could be due to the ICT.[6,43] This is fully in accord with our calculations and results, the absorption maximum for **poly-3e** at 540 nm indicative of a low molecular weight poly(terthiophene), with the broad absorption at 778 nm due to a ICT band. It has also been reported that compounds with donor−acceptor substituents at the terminal positions exhibit a large bathochromic shift, which results from intramolecular charge transfer.[44] Interestingly, the absorption maximum for undoped polyterthiophene itself is at 400 nm,[45] supporting the activating effect of the alkoxy groups toward longer chain polymerization.

The low molecular weight obtained for **poly-3e** is fully consistent with our previous observations on the polymerization of similar unsubstituted styrylterthiophenes for which we have conclusively demonstrated that oxidative polymerization of these types of functionalized terthiophenes is limited to dimerization, as a result of the pinning of the dimer polaron restricting further chain growth.[46] While this will be ameliorated to some extent by the activating effect of the alkoxy substituents, the styryl-like indanedione substituent apparently dominates the monomer reactivity leading to shorter chain polymers.

As the **poly-3e** film is oxidized, the ICT band loses intensity. The detailed nature of the positive polaron spectrum will depend on the effective conjugation length of the polymers of interest; however, a crude model of the polaron may be gleaned from calculations of the oxidized monomer species, i.e., $\mathbf{3}^+$. The TDDFT calculations on $\mathbf{3}^+$ reveal that the spectrum is significantly different from that of **3** with strong absorption features present in the red and near-IR region and the disappearance of the ICT band. These calculations are consistent with the observed spectroelectrochemical data.

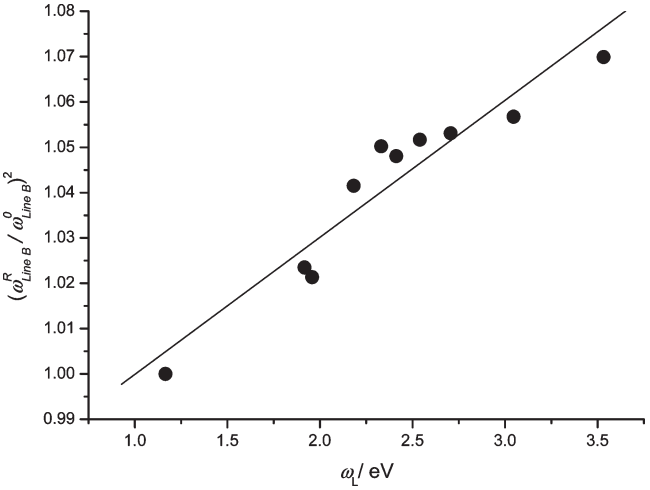

Figure 5. Frequency dispersion data for **poly-3e**. The plot relates the frequency of line B (ω^R_{LineB}) as a function of laser excitation frequency (ω_L) under resonance conditions with the nonresonant frequency of line B (ω^0_{LineB}) against laser excitation frequency.

The phenomenon of Raman frequency dispersion, in that a polymer backbone vibrational mode (line B[36,37]) appears to shift with excitation wavelength, may provide insight into the effective conjugation length in polymer species, which can be related to conductivity and optical properties.[47,48] The rationale for the apparent shifting of polymer backbone bands with excitation wavelength is that the polymer is made up of domains with differing effective conjugation lengths, which come into resonance at differing excitation frequencies and possess slightly different backbone vibrational frequencies.[37] We have examined the resonance Raman spectra of oxidized **poly-3e** and find that there is a frequency dispersion effect on the line B polythiophene band (Figure 5).[49,50] A common way to parametrize these data is a plot of the dispersion rate parameter D.[47] For **poly-3e** value of 0.03 eV^{-1} is obtained for D. This is similar to the value of 0.02 eV^{-1} reported for polythiophene and indicates that the conjugation length in **poly-3e** is not significantly different from that in the parent unsubstituted polymer. This is supportive of the charge transfer nature of the low-band-gap transition. As such a transition involves the isolated indanedione moiety, it cannot contribute to extending the polymer backbone effective conjugation length.

The optical band gap energy E_g^{opt} of the polymers can be estimated from the absorption band edge.[4,51] The optical band gap, E_g^{opt}, for **poly-2e** and **poly-3e** were calculated to be 1.0 and 1.1 eV respectively, significantly lower than for other polythiophenes.[4] Assuming that the ICT band can be utilized for light harvesting, these polymers provide exciting opportunities for organic solar cells.

In order to obtain free-standing films for conductivity measurements, both **poly-2e** and **poly-3e** were grown on ITO-coated glass by chronoamperometric deposition at a constant potential of 0.9 V for 1 h. The conductivity of **poly-2e** was 1.8 S/cm, which is similar to that of **poly-3e** (1.1 S/cm), demonstrating that the longer alkoxy side chains of **poly-3e** do not dramatically impact on the conductivity. The conductivities are, however, an order of magnitude higher than that reported by Gallazzi et al. for an analogous poly(alkoxyterthiophene) substituted with the somewhat smaller electron-withdrawing dicyanoethenyl group,[7] suggesting that the larger indandione group enhances interchain conductivity.

The morphologies of the electrochemically **poly-3e** films were analyzed by SEM, and the images are shown in Figure S4.

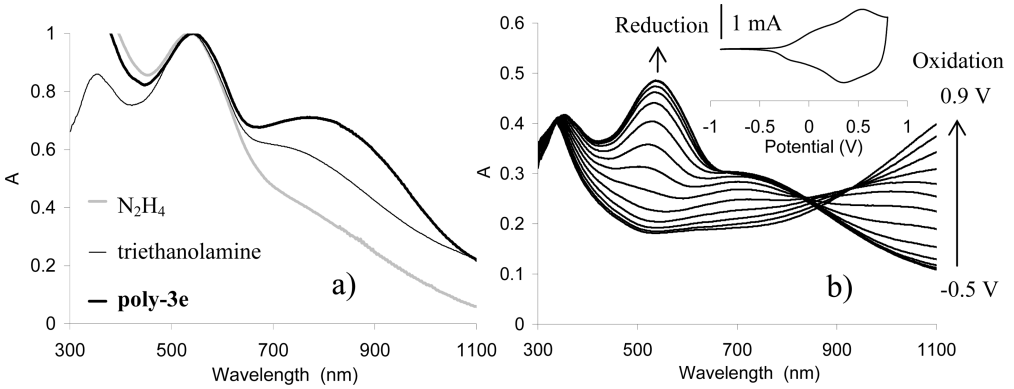

Figure 6. Normalized spectra for (a) **poly-3c** electrochemically reduced after chemical reduction with hydrazine, triethanolamine, and the electrochemically reduced spectrum from **poly-3e**; (b) spectroelectrochemistry of a **poly-3c** film (inset: post CV at 100 mV/s).

Scheme 2. Mechanism for the Formation of Diimine 7

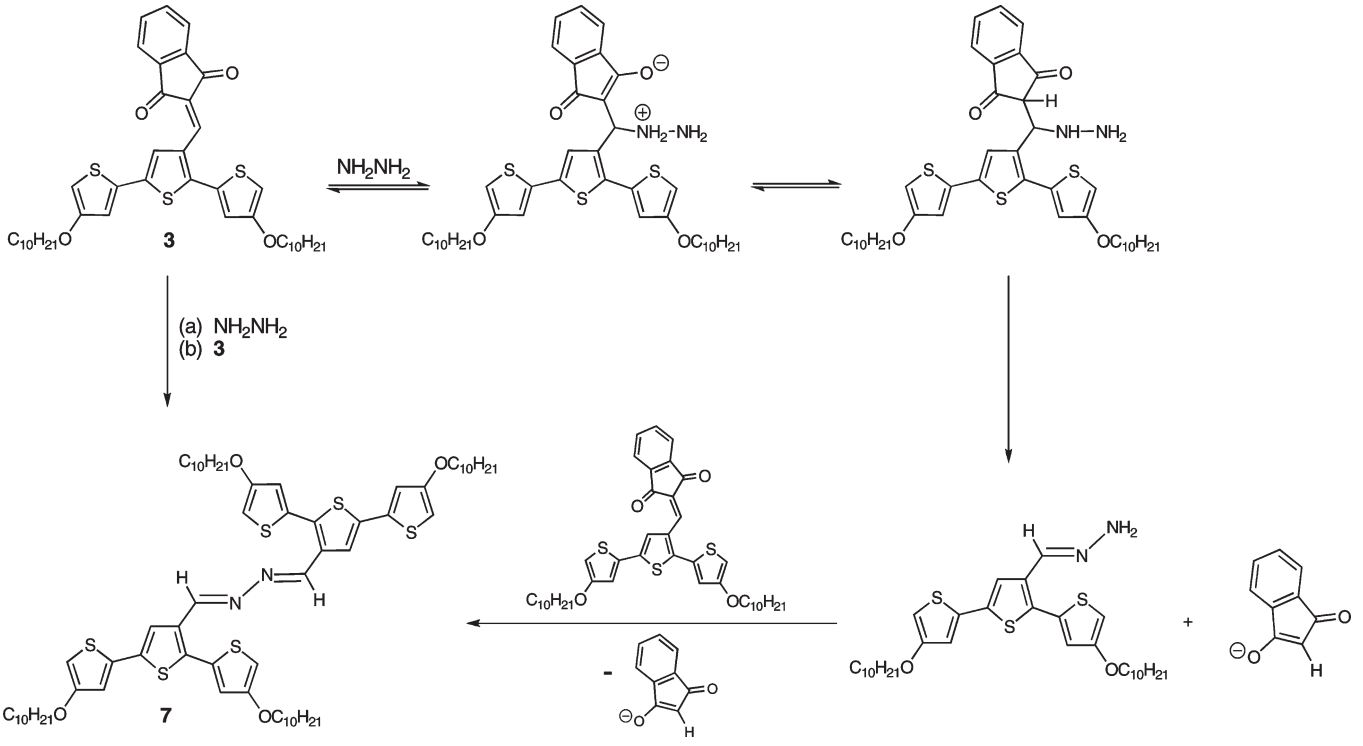

The very wrinkled nature of the film is atypical of substituted poly(terthiophene) films.[52] This morphology may reflect both the bulky nature of the substituent as well as the dual growth mechanism proposed by Schrebler et al.[53] Formation of an initial flat film firmly adhered to the electrode surface by 2D nucleation and growth (dense film, Figure S4a), followed by oxidative swelling (3D growth), may account for this film wrinkling. Trapped solvent or nucleated gases may also contribute to this unusual morphology.

Chemical Polymer Synthesis and Characterization. Given the previous finding that there was little difference in the electrochemical properties between the **poly-2e** and **poly-3e**, only the chemical polymerization of the decyloxy-substituted indanedione terthiophene **3** was investigated. The monomer **3** was oxidized with ferric chloride at low temperature under argon using a well-established oxidation procedure.[41] In order to isolate the resulting polythiophene, the crude oxidized polymer was initially reduced with hydrazine and the neutral polymeric mixture subjected to solvent fractionation. The resulting chloroform fraction yielded only a small amount of polymeric material, which was electrochemically reduced in order to compare it to **poly-3e**. The UV−vis spectral comparison is shown in Figure 6a. It was apparent that, while a band attributed to the polythiophene backbone (540 nm) and similar to that observed in the electrochemically polymerized **poly-3e** spectrum was evident, the longer wavelength ICT band at 780 nm was significantly diminished. This implied that the indanedione group had been affected in some way either during chemical oxidation or reduction.

In order to clarify this, the reaction of monomer **3** with hydrazine was investigated and resulted in the isolation of a bright red product, whose ^{1}H NMR spectrum revealed a complete absence of indanedione aromatic resonances. This apparent loss of the indanedione moiety was confirmed by MALDI mass spectrometry, which gave mass data (*m*/*z* 1172) corresponding to the diimine-linked bis-alkoxyterthiophene structure **7** (Scheme 2).

A fragment peak at *m*/*z* 586 corresponds to half this structure. The ^{1}H NMR spectrum of **7** (Figure S5) is fully

Table 2. Results from the Chemical Reduction of Oxidized by $FeCl_3$: Poly-3c, Poly-3/6, and Poly-6

method	monomer **3**, mg	monomer **6**, mg	polymer	polymer, mg (yield, %)	M_w (Da)	PDI
EtOH	58.8		**poly-3c**	8.1 (13.8)	3300	1.8
formaldehyde/PhCl	51.2		**poly-3c**	21.6 (42.2)	4300	1.4
triethanolamine/PhCl	50.4		**poly-3c**	34.0 (68.0)	4500	1.5
triethanolamine/PhCl	24.8	25.4	**poly-3/6**	34.2 (68.0)	20400	2.6
triethanolamine/PhCl		49.4	**poly-6**	39.6 (80.0)	91300	1.8

consistent with this structure, with the vinylic proton resonance at 8.64 ppm in the monomer **3** shifted to 8.87 ppm as expected for an imine proton and the three remaining aromatic signals and multiplet consistent with a 3-substituted dialkoxyterthiophene. Imine **7** presumably arises by initial conjugate addition of hydrazine to the double bond followed by elimination of indanedione itself (Scheme 2). Repetition of this leads to the diimine **7**. The same reaction presumably occurs during the reduction of oxidized **poly-3c**, and therefore alternative reducing agents were investigated, initially ascertaining the stability of monomer **3** toward the reducing agent.

We investigated the use of mild to moderately strong reducing agents such as ammonium hydroxide, ethanol, formaldehyde, ethanolamine, and triethanolamine that have all been used previously for nanoparticle synthesis.[54] Both ammonium hydroxide and ethanolamine reacted with monomer **3** to varying degrees to give terthiophene aldehyde **1b** ($R = C_{10}H_{21}$) rather than the diimine **7** (Scheme 2), whereas it appeared stable to the other three reductants, and the reduction of oxidized **poly-3c** was undertaken using these three reagents.

Polymer Reduction. The reduction of the oxidized **poly-3c** was investigated using ethanol, formaldehyde, triethanolamine, and the results given in Table 2. During reduction, chloroform and chlorobenzene were used to increase the solubility and thus accessibility of the polymer to the reducing agent.

The highest yield of $CHCl_3$-soluble polymer was obtained using triethanolamine and chlorobenzene. Oxidative polymerization of **3** followed by triethanolamine reduction and chloroform extraction resulted in a 68% yield of **poly-3c**, with a weight-average molecular weight of 4500 Da and a PDI of 1.5. This corresponds to a chain length of six indanedione terthiophene monomer units (4292 Da). The remaining longer chain material remained insoluble in conventional organic solvents. To the best of our knowledge, this is the first time that the use of triethanolamine for the reduction of an oxidized polythiophene has been reported, providing the conducting polymer chemist with a milder and safer alternative to hydrazine.

The UV−vis solution spectrum of **poly-3c** after triethanolamine reduction now exhibited a broad band between 600 and 1300 nm that appeared to be two overlapping bands, a ICT band at 740 nm, and a second longer wavelength band at 885 nm (Figure S6), which can be attributed to the presence of polarons in the polymer, suggesting incomplete reduction by triethanolamine. This was confirmed by the complete disappearance of the band at 885 nm on electrochemically reducing a dip-coated film of **poly-3c** on an ITO electrode (Figure 6a,b). The UV−vis spectrum of this film is almost identical to that of **poly-3e** (Figure 6a), except for a loss in intensity of the ICT band and the absorbance at 340 nm. While the reason for this loss in intensity is not obvious, the ^{1}H NMR spectra of the **poly-3c** (Figure 1b) provides some insight into this.

As expected for a regioirregular polymer, the ^{1}H NMR signals of **poly-3c** are broadened as in Figure 1b but still agree closely with the monomer spectrum (Figure 1a). The aromatic proton signals from the indanedione moiety are still present at 7.7−8.2 ppm, and the signal at 6.2 ppm attributed to the protons alpha to the sulfur atoms has disappeared, indicating chain formation. Most notably, a shift of the $H_{4'}$ signal is still observed in the homopolymer ^{1}H NMR spectrum, indicating the retention of charge transfer behavior upon polymerization. Nonetheless, a sizable signal at ~7.5 ppm is present, indicating that some 4′ protons are unaffected by the indanedione carbonyl group and suggesting that there is disruption of the indanedione conjugation. This may account for the loss in the ICT band intensity in the UV−vis spectra.

The full spectroelectrochemistry for a solvent cast **poly-3c** film is shown in Figure 6b along with the polymer post CV. When compared to the spectroelectrochemistry of **poly-3e** (Figure 4), this data highlights the differences in length and conjugation of these polymers. In particular, the post CVs show quite distinct changes in peak current associated with each redox process. The less positive peak in the post CV of polythiophenes can be ascribed to oxidation of long chain polymer segments, while the more positive one originates from oxidation of short-chain zones of the film.[40] According to this interpretation, the contribution of the short-chain segments in **poly-3c** are higher than in **poly-3e**, suggesting that the chain length of **poly-3e** is somewhat longer than the six terthiophene units of **poly-3c**. It is worthy of note that for both **poly-3e** and **poly-3c** the ICT band is fully recoverable on potential cycling. Cycling of both films between −0.5 and 0.9 V a number of times does not lead to any discernible change in the absorption spectra of the reduced and oxidized films.

Chemical Copolymerization. The cast films of **poly-3c** were quite brittle in nature, reflecting the low molecular weight of the polymer. Therefore, in order to increase the polymer molecular weight and improve the processability of the indanedione-substituted poly(terthiophene)s, making layer deposition via conventional spin-coating methods possible, chemical copolymerization of the indanedione-substituted terthiophene with a terthiophene monomer was investigated.

An identical procedure to that used for the homopolymerization of **3**, employing triethanolamine as reducing agent, was utilized to effect the copolymerization of a 1:1 mixture of indanedione terthiophene **3** and dihexylterthiophene **6**, and the resulting copolymer, **poly-3/6**, was obtained in 68% yield (Scheme 1). For comparison, the homopolymer **poly-6** of dihexylterthiophene **6** was also prepared in 80% yield by the same procedure.

The FT-IR spectra of **poly-3c** and **poly-3/6** both exhibit a pair of stretches at 1682 and 1722 cm^{-1}, corresponding to the carbonyl stretches of the indanedione moiety. These stretches are absent in the spectrum of **poly-6** as expected (Figure 7).

The ^{1}H NMR spectrum of **poly-3/6** (Figure S7) displays unique signals from both monomers, arising from the charge transfer shifted hydrogen on the central thiophene ring of **3** (8.6 ppm) and the four hydrogens of the two hexyl chains directly adjacent to the central thiophene unit of **6** (2.8 ppm). Integrations of these signals revealed that the actual copolymer composition ratio of indanedione-TTh **3** to dihexyl-TTh **6** was 1:3.

The absorbance spectrum of **poly-3/6** (Figure S8) appeared as a combination of the absorbances characteristic

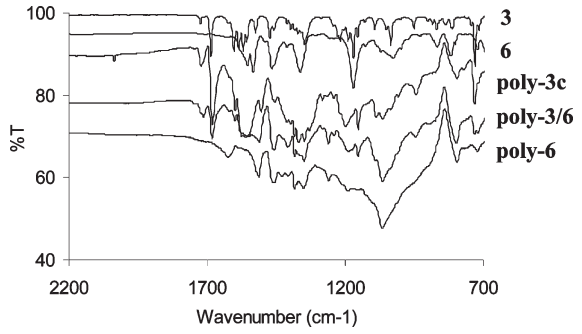

Figure 7. FT-IR spectra of monomers and chemically polymerized homopolymers and copolymer.

of the two homopolymers, **poly-3c** and **poly-6**, the indanedione-TTh polymer and the dihexyl-TTh polymer, respectively, with maxima at 360 and 507 nm, although no charge transfer band at 780 nm was apparent. However, this is not surprising given that the charge transfer band in the indanedione terthiophene monomer **3** is at 471 nm. The indanedione terthiophene unit in **poly-3/6** is effectively isolated in the 1:3 copolymer and therefore might be expected to have similar spectroscopic characteristics to the monomer **3** itself. Since the polythiophene backbone absorption of **poly-3/6** is at 523 nm, the charge transfer band will be masked. Nonetheless, the ^{1}H NMR proton signal at 8.6 ppm supports the presence of the ICT interaction.

As was observed for **poly-3c**, triethanolamine did not completely reduce the polymers. Reduced **poly-3/6** and **poly-6** both exhibit absorbance peaks at roughly 900 nm (Figure S8). Doping **poly-3/6** with $Cu(ClO_4)_2$ resulted in the loss of the absorbance at 507 nm and produced a free carrier tail past 1000 nm, indicative of an electroactive polymer. Similar behavior was observed for **poly-6**.

The copolymer **poly-3/6** exhibited a significantly higher molecular weight than **poly-3c**, although the polydispersity increased somewhat (Table 2). This reflects the excellent solubilizing capability of the dihexylterthiophene as evidenced by the high molecular weight (91 300 Da) of the homopolymer **poly-6** (Table 2). The copolymer also was more elastic in nature and less brittle than **poly-3c**, indicating that it may be suitable for spin-coating in device fabrication. Studies in this regard are ongoing.

Conclusions

A poly(terthiophene) **poly-3e** exhibiting charge transfer characteristics due to the presence of an indanedione substituent was electrochemically polymerized. The resulting intramolecular charge transfer (ICT) band in reduced **poly-3e** considerably expands the light absorption characteristics of this polythiophene. While the band is lost upon oxidation, it is completely restored on re-reduction. Insights into the electronic nature of the ICT band of **poly-3e** were obtained from DFT calculations and Raman spectroscopy of indanedione-substituted monomers. While **poly-3e** has potential as a broad band light harvester in photovoltaic applications, it is suffers from a lack of processability.

A similar oxidized polymer could be chemically prepared but reduction with hydrazine destroyed the indanedione substituent. The use of a milder reducing agent, triethanolamine, permitted the isolation of soluble **poly-3c**, which exhibited a charge transfer band in its absorbance spectrum almost identical to that of **poly-3e**. However, **poly-3c** produced a brittle film due to its low molecular weight (4500 Da).

Copolymerizations with a dihexyl-TTh monomer both increased the molecular weight of the resulting polymer as well as improved the polymer solubility, yielding a more elastic, although polydisperse, material, **poly-3/6**. While this copolymer retains charge transfer characteristics, they more closely resemble those of the indanedione-substituted monomer.

Nonetheless, we have demonstrated that a processable polythiophene with a significant intramolecular charge transfer band, albeit with a low molecular weight, can be prepared, and this material has exciting potential for exploring the use of ICT bands in photovoltaic applications for extending light harvesting into the red.

Acknowledgment. This work was supported by the Australian Research Council, the MacDiarmid Institute for Advanced Materials and Nanotechnology, New Zealand Foundation for Research, Science and Technology, and New Zealand International Investment Opportunities Fund Contract CO8X0602.

Note Added after ASAP Publication. Due to a production error, this paper was originally published with minor errors in the text on March 26, 2010. The corrected version was reposted on April 2, 2010.

Supporting Information Available: Figures showing the computed structure of indanedione-substituted terthiophene **3**, molecular orbitals for indanedione-substituted terthiophene **4**, Lippert−Mataga plot for **4**, SEM images of electrochemically polymerized **poly-3e**, ^{1}H NMR and ^{13}C NMR spectra of diimine-linked bis-alkoxyterthiophene **7**, UV−vis spectra of **poly-3c**, **poly-6**, and **poly-3/6**, and the ^{1}H NMR spectra of copolymer **poly-3/6**. This material is available free of charge via the Internet at http://pubs.acs.org.

References and Notes

(1) Roncali, J. *Chem. Rev.* **1992**, *92*, 711–38.
(2) Li, Y.; Zou, Y. *Adv. Mater.* **2008**, *20*, 2952–2958.
(3) Ahn, S.-H.; Czae, M.-z.; Kim, E.-R.; Lee, H.; Han, S.-H.; Noh, J.; Hara, M. *Macromolecules* **2001**, *34*, 2522–2527.
(4) Roncali, J. *Chem. Rev.* **1997**, *97*, 173–205.
(5) Zhang, Q. T.; Tour, J. M. *J. Am. Chem. Soc.* **1998**, *120*, 5355–5362.
(6) Casalbore-Miceli, G.; Gallazzi, M. C.; Zecchin, S.; Camaioni, N.; Geri, A.; Bertarelli, C. *Adv. Funct. Mater.* **2003**, *13*, 307–312.
(7) Gallazzi, M. C.; Toscano, F.; Paganuzzi, D.; Bertarelli, C.; Farina, A.; Zotti, G. *Macromol. Chem. Phys.* **2001**, *202*, 2074–2085.
(8) Roquet, S.; Cravino, A.; Leriche, P.; Aleveque, O.; Frere, P.; Roncali, J. *J. Am. Chem. Soc.* **2006**, *128*, 3459–66.
(9) Zhu, Y.; Champion, R. D.; Jenekhe, S. A. *Macromolecules* **2006**, *39*, 8712–8719.
(10) Wagner, P.; Officer, D. L. *Synth. Met.* **2005**, *154*, 325–328.
(11) Gallazzi, M. C.; Castellani, L.; Marin, R. A.; Zerbi, G. *J. Polym. Sci., Part A: Polym. Chem.* **1993**, *31*, 3339–49.
(12) Wen, S.; Pei, J.; Zhou, Y.; Li, P.; Xue, L.; Li, Y.; Xu, B.; Tian, W. *Macromolecules* **2009**, *42*, 4977–4984.
(13) Keegstra, M. A.; Brandsma, L. *Synthesis* **1988**, *11*, 890–1.
(14) Gallazzi, M. C.; Castellani, L.; Zerbi, G.; Sozzani, P. *Synth. Met.* **1991**, *41*, 495–8.
(15) Collis, G. E.; Burrell, A. K.; Scott, S. M.; Officer, D. L. *J. Org. Chem.* **2003**, *68*, 8974–83.
(16) Clarke, T. M.; Gordon, K. C.; Chan, W. S.; Phillips, D. L.; Wagner, P.; Officer, D. L. *ChemPhysChem* **2006**, *7*, 1276–1285.
(17) Clarke, T. M.; Gordon, K. C.; Officer, D. L.; Hall, S. B.; Collis, G. E.; Burrell, A. K. *J. Phys. Chem. A* **2003**, *107*, 11505–11516.
(18) Clarke, T. M.; Gordon, K. C.; Officer, D. L.; Grant, D. K. *J. Chem. Phys.* **2006**, *124*, 164501/1–164501/11.
(19) Clarke, T. M.; Gordon, K. C. *J. Mol. Struct.: THEOCHEM* **2007**, *815*, 135–143.
(20) Earles, J. C.; Gordon, K. C.; Officer, D. L.; Wagner, P. *J. Phys. Chem. A* **2007**, *111*, 7171–7180.
(21) Lind, S. J.; Gordon, K. C.; Gambhir, S.; Officer, D. L. *Phys. Chem. Chem. Phys.* **2009**, *11*, 5598–5607.
(22) Cleland, D. M.; Irwin, G.; Wagner, P.; Officer, D. L.; Gordon, K. C. *Chem.—Eur. J.* **2009**, *15*, 3682–3690.

(23) Lundin, N. J.; Walsh, P. J.; Howell, S. L.; Blackman, A. G.; Gordon, K. C. *Chem.—Eur. J.* **2008**, *14*, 11573–11583.
(24) Waterland, M. R.; Flood, A.; Gordon, K. C. *J. Chem. Soc., Dalton Trans.* **2000**, *2*, 121–127.
(25) Lind, S. J.; Walsh, T. J.; Blackman, A. G.; Polson, M. I. J.; Irwin, G. I. S.; Gordon, K. C. *J. Phys. Chem. A* **2009**, *113*, 3566–3575.
(26) Lind, S. J.; Gordon, K. C.; Waterland, M. R. *J. Raman Spectrosc.* **2008**, *39*, 1556–1567.
(27) Iwao, M.; Lee, M. L.; Castle, R. N. *J. Heterocycl. Chem.* **1980**, *17*, 1259–64.
(28) Melucci, M.; Frere, P.; Allain, M.; Levillain, E.; Barbarella, G.; Roncali, J. *Tetrahedron* **2007**, *63*, 9774–9783.
(29) Clarke, T. M.; Gordon, K. C.; Kwok, W. M.; Phillips, D. L.; Officer, D. L. *J. Phys. Chem. A* **2006**, *110*, 7696–7702.
(30) Ortiz, R. P.; Gonzalez, S. R.; Casado, J.; Navarrete, J. T. L.; Officer, D. L.; Wagner, P.; Earles, J. C.; Gordon, K. C. *ChemPhysChem* **2009**, *10*, 1901–1910.
(31) Lakowicz, J. R. *Principles of Fluorescence Spectroscopy*; Kluwer Academic: New York, 1999.
(32) Mataga, N.; Karen, A.; Okada, T.; Nishitani, S.; Kurata, N.; Sataka, Y.; Misumi, S. *J. Am. Chem. Soc.* **1984**, *106*, 2442–3.
(33) Kamlet, M. J.; Abboud, J. L.; Taft, R. W. *J. Am. Chem. Soc.* **1977**, *99*, 6027–6038.
(34) Huss, A. S.; Pappenfus, T.; Bohnsack, J.; Burand, M.; Mann, K. R.; Blank, D. A. *J. Phys. Chem. A* **2009**, *113*, 10202–10210.
(35) Hirakawa, A. Y.; Tsuboi, M. *Science* **1975**, *188*, 359–61.
(36) This very strong mode in the Raman spectrum of **4** corresponds to the polythiophene mode at approximately the same frequency. This feature is called line B, and its behavior as a function of excitation wavelength reveals some sign of the nature of the effective conjugation length in polymer systems (vida infra).
(37) Jadamiec, M.; Lapkowski, M.; Officer, D. L.; Wagner, P.; Gordon, K. C. *Int. J. Nanotechnol.* **2009**, *6*, 344–354.
(38) Gambhir, S.; Wagner, K.; Officer, D. L. *Synth. Met.* **2005**, *154*, 117–120.
(39) Chen, X.; Inganaes, O. *J. Phys. Chem.* **1996**, *100*, 15202–15206.
(40) Skompska, M. *Electrochim. Acta* **1998**, *44*, 357–362.
(41) Skotheim, T. A., Reynolds, J. R., Eds.; *Handbook of Conducting Polymers*, 3rd ed.; CRC Press: Boca Raton, FL, 2007.
(42) Groenendaal, L. B.; Zotti, G.; Aubert, P.-H.; Waybright, S. M.; Reynolds, J. R. *Adv. Mater.* (*Weinheim, Ger.*) **2003**, *15*, 855–879.
(43) Casalbore-Miceli, G.; Camaioni, N.; Geri, A.; Ridolfi, G.; Zanelli, A.; Gallazzi, M. C.; Maggini, M.; Benincori, T. *J. Electroanal. Chem.* **2007**, *603*, 227–234.
(44) Meier, H. *Angew. Chem., Int. Ed.* **2005**, *44*, 2482–2506.
(45) Roncali, J.; Garnier, F.; Lemaire, M.; Garreau, R. *Synth. Met.* **1986**, *15*, 323–31.
(46) Grant, D. K.; Jolley, K. W.; Officer, D. L.; Gordon, K. C.; Clarke, T. M. *Org. Biomol. Chem.* **2005**, *3*, 2008–2015.
(47) Millen, R. P.; de Faria, D. L. A.; Temperini, M. L. A. *Synth. Met.* **2006**, *156*, 459–465.
(48) Heller, C.; Leising, G.; Godon, C.; Lefrant, S.; Fischer, W.; Stelzer, F. *Phys. Rev. B* **1995**, *51*, 8107–8114.
(49) Furukawa, Y. *J. Phys. Chem.* **1996**, *100*, 15644–15653.
(50) Furukawa, Y. *Handb. Adv. Electron. Photonic Mater. Devices* **2001**, *8*, 303–320.
(51) Gierschner, J.; Cornil, J.; Egelhaaf, H.-J. *Adv. Mater.* (*Weinheim, Ger.*) **2007**, *19*, 173–191.
(52) Dini, D.; Decker, F.; Andreani, F.; Salatelli, E.; Hapiot, P. *Polymer* **2000**, *41*, 6473–6480.
(53) Schrebler, R.; Grez, P.; Cury, P.; Veas, C.; Merino, M.; Gomez, H.; Cordova, R.; del Valle, M. A. *J. Electroanal. Chem.* **1997**, *430*, 77–90.
(54) Rao, C. R. K.; Trivedi, D. C. *Synth. Met.* **2005**, *155*, 324–327.